



**HAL**  
open science

## A Methodology For 3d Nonlinear Soil-Structure Interaction Using The Domain Reduction Method

Michail Korres, Filippo Gatti, Vinicius Alves Fernandes, F Lopez-Caballero, Irmela Zentner, François Voltaire

► **To cite this version:**

Michail Korres, Filippo Gatti, Vinicius Alves Fernandes, F Lopez-Caballero, Irmela Zentner, et al.. A Methodology For 3d Nonlinear Soil-Structure Interaction Using The Domain Reduction Method. 17th World Conference on Earthquake Engineering, 17WCEE, Sep 2020, Sendai (Japan), Japan. pp.1-12. hal-04680636

**HAL Id: hal-04680636**

**<https://hal.science/hal-04680636v1>**

Submitted on 28 Aug 2024

**HAL** is a multi-disciplinary open access archive for the deposit and dissemination of scientific research documents, whether they are published or not. The documents may come from teaching and research institutions in France or abroad, or from public or private research centers.

L'archive ouverte pluridisciplinaire **HAL**, est destinée au dépôt et à la diffusion de documents scientifiques de niveau recherche, publiés ou non, émanant des établissements d'enseignement et de recherche français ou étrangers, des laboratoires publics ou privés.



## A METHODOLOGY FOR 3D NONLINEAR SOIL-STRUCTURE INTERACTION USING THE DOMAIN REDUCTION METHOD

M. Korres<sup>(1)</sup>, F. Gatti<sup>(2)</sup>, V. Alves Fernandes<sup>(3)</sup>, F. Lopez-Caballero<sup>(4)</sup>, I. Zentner<sup>(5)</sup>, F. Voldoire<sup>(6)</sup>

<sup>(1)</sup> PhD student, *Électricité de France-R&D Department, [michail.korres@edf.fr](mailto:michail.korres@edf.fr) and CentraleSupélec, Laboratoire Mécanique des Sols, Structures et Matériaux (MSSMat) UMR CNRS 8579, [michail.korres@centralesupelec.fr](mailto:michail.korres@centralesupelec.fr)*

<sup>(2)</sup> Assistant professor, *CentraleSupélec, Laboratoire Mécanique des Sols, Structures et Matériaux (MSSMat) UMR CNRS 8579, [filippo.gatti@centralesupelec.fr](mailto:filippo.gatti@centralesupelec.fr)*

<sup>(3)</sup> Research engineer, *Électricité de France-R&D Department and IMSIA UMR EDF-CNRS-CEA ENSTA 9219, [vincius.alves-fernandes@edf.fr](mailto:vincius.alves-fernandes@edf.fr)*

<sup>(4)</sup> Associate professor, *CentraleSupélec, Laboratoire Mécanique des Sols, Structures et Matériaux (MSSMat) UMR CNRS 8579, [fernando.lopez-caballero@centralesupelec.fr](mailto:fernando.lopez-caballero@centralesupelec.fr)*

<sup>(5)</sup> Expert research engineer, *Électricité de France-R&D Department and IMSIA UMR EDF-CNRS-CEA ENSTA 9219, [irmela.zentner@edf.fr](mailto:irmela.zentner@edf.fr)*

<sup>(6)</sup> Senior expert research engineer, *Électricité de France-R&D Department and IMSIA UMR EDF-CNRS-CEA ENSTA 9219, [francois.voldoire@edf.fr](mailto:francois.voldoire@edf.fr)*

### Abstract

Soil-structure interaction (SSI) consists of an important step on the evaluation of seismic response of structures and equipment of nuclear power plants. In the current engineering practice, strong hypothesis such as vertical incidence plane waves with equivalent lateral boundaries and horizontal soil stratification is usually adopted so as to simplify the SSI studies. However, in reality, the incident wave field to be applied as an input excitation is more complex. Thus, it is necessary to properly model the complete wave propagation problem from the source to the site of interest which could be a computationally costly procedure. A good compromise between the accuracy and efficiency from a computational point of view is examined in this work.

For this purpose, a weak coupling approach based on the domain reduction (DRM) introduced by Bielak et al. [1] is used in this work. The definition of a 3D complex incident wave is provided through a spectral element method. It is used so as to study wave propagation from source to site in a regional scale model. Then, the 3D incident wave field is then injected in a finite element code (`code_aster`) so as to study the response of a reduced domain model in a more accurate way. The aim of this paper is to verify the weak coupling methodology implemented in `code_aster` for some cases related with i) the used soil behavior and ii) the mesh conformity between both numerical codes. The case-studies are the ones of the PRENOLIN benchmark and the canonical case CAN4.

For cases of strong ground motion, soil behavior plays a major role, thus, the impact of a nonlinear soil response is examined in the finite element framework so as to evaluate the efficiency of the DRM approach treating this kind of studies. To represent the structure, the well-known case of Kashiwazaki-Kariwa nuclear power plant is used. In addition, a modification of the sedimentary basins' geometry is proposed so as to study the consequences of surface waves propagation in the efficiency of the DRM methodology.

It is showed that the implemented methodology in `code_aster` provides a good approximation of the whole system response when the DRM approach is used.

*Keywords: nonlinear SSI; domain reduction method; weak coupling SEM - FEM;*



## 1. Introduction

Soil-structure interaction (SSI) consists of an important step on the evaluation of seismic response of structures and equipment of nuclear power plants. Two of the major uncertainties could be related with i) soil behavior representation, and ii) the definition of the input seismic loading amongst others. Concerning the first point, the current engineering practice consists in adopting an equivalent linear elastic constitutive law for the soil and a linear elastic behavior for the structural elements, even though several authors considered soil and structural nonlinear behavior considering SSI studies ([2]–[6] amongst others). In most of these studies different nonlinear constitutive laws are chosen to model soil as well as structure behavior, while in some of them mechanical characteristics of the soil media as well as seismic excitations are taken into account in a probabilistic framework ([7], [8]).

The definition of this seismic excitation as an input to the numerical SSI studies is supposed to be a plane wave with vertical incidence. However, in reality, the incident wave field to be applied as an input excitation is more complex. Thus, it is necessary to properly model the complete wave propagation problem from the source to the site of interest which could be a computationally costly procedure. A good compromise between the accuracy and efficiency from a computational point of view is the domain reduction method (DRM) methodology that was initially introduced by Bielak et al. [1]. It allows to express the complete incident wave field in terms of equivalent nodal forces exerted at the boundaries of a reduced domain enclosing the structure of interest. In this context and based on the DRM theory, the scope of this work is to verify the implementation of a weak coupling between a spectral element (SEM3D [9]) and finite element (code\_aster [10]) code, so as to ensure the application of a more realistic incident seismic wave field as an input to the nonlinear SSI studies. An initial verification of the method without structure and only for soil linear elastic behavior is presented at first, by reference to a complete 3D wave propagation with SEM3D. Two case-studies are considered in this framework in order to examine different aspects of the weak coupling approach. The first case-study is the PRENOLIN benchmark [11] where a simple horizontally-layered soil geometry and seismic excitation are taken into consideration. Then a more complex basin geometry and seismic excitation are considered for the canonical case CAN4 [12].

The nonlinear SSI model is then examined in a finite element framework (FEM) with code\_aster. The current implementation of the DRM approach in code\_aster uses zero-order absorbing paraxial elements [13] so as to compute and apply the equivalent nodal forces on the boundary of the reduced domain; which is validated for a linear soil behavior [14]. For the case where the nonlinear soil behavior is induced, an important contrast on the impedance ratio between the soil and the surface where the forces are imposed may appear. It could generate spurious reflections, which are related principally to the absorbing boundary conditions of the DRM. Consequently, the efficiency of the current implementation of the DRM approach is evaluated using a simplified nonlinear constitutive behavior of the soil (i.e. Iwan's [15] model). The non-linear SSI analysis is performed considering Unit 7 Kashiwasaki-Kariwa Nuclear Power Plant reactor building response during the 2007 Niigata Chuetsu-Oki earthquake mainshock, which was the object of the former international benchmark Karisma [16]. Finally, a modification of the sedimentary basins' geometry is proposed so as to study the consequences of surface waves propagation in the efficiency of the DRM methodology.

## 2. Domain Reduction Method

### 2.1 Theoretical background

The Domain Reduction Method (DRM) methodology, initially proposed by Bielak et al. [1], consists of a two-step dynamic procedure that splits the initial problem (Fig. 1a) in two separate independent problems. The first one is an auxiliary domain problem (Fig. 1b), where wave propagation from source to the site is studied in order to compute the equivalent nodal forces on the boundary  $\Gamma$  of a reduced domain of interest  $\Omega$ . In order to decrease the computational cost of this first step that can be solved for a large-scale (regional) model, the geology of interest, domain  $\Omega$ , is replaced by a simplified geology  $\Omega^0$  which allows for a larger element size



and thus a smaller model in terms of degrees of freedom (dof) and phenomenology involvement. The second step consists of the reduced domain problem (Fig. 1c) where only the reduced domain  $\Omega$  is taken into consideration, while the seismic excitation is now expressed in terms of equivalent nodal forces computed on the first step of the dynamic procedure.

The mathematical expression proposed by Bielak et al. [1] for the computation of the equivalent nodal forces  $\mathbf{F}_{eq}$  is derived from the Navier's equation for elastodynamics and is given with Eq. (1) :

$$\mathbf{F}_{eq} = \begin{Bmatrix} \mathbf{F}_{eq}^i \\ \mathbf{F}_{eq}^b \\ \mathbf{F}_{eq}^e \end{Bmatrix} = \begin{Bmatrix} 0 \\ -\mathbf{M}_{be}^{\Omega^+} \ddot{\mathbf{u}}_e^0 - \mathbf{K}_{be}^{\Omega^+} \mathbf{u}_e^0 \\ \mathbf{M}_{eb}^{\Omega^+} \ddot{\mathbf{u}}_b^0 + \mathbf{K}_{eb}^{\Omega^+} \mathbf{u}_b^0 \end{Bmatrix} \quad (1)$$

where,  $\mathbf{u}^0, \ddot{\mathbf{u}}^0$  are the displacement and acceleration field in the auxiliary problem,  $\mathbf{M}, \mathbf{K}$  are the mass and stiffness matrices and the indexes  $i, e, b$  stand for the 3 domains: i) interior, ii) exterior, and iii) boundary  $\Gamma$  (Fig. 1a). Based on Eq. (1), in order to compute the equivalent nodal forces it suffices to know the displacement and acceleration field in the auxiliary problem only in a one element layer of the boundary (Fig. 1c). In the initial formulation of the method, the domain  $\hat{\Omega}^+$  (Fig. 1c) located outside the boundary  $\Gamma$  where the equivalent nodal forces are applied, is proposed to be used as an absorbing layer for the scattered waves that arriving on the boundary. For more details about the equations and hypothesis of this method, refer to Bielak et al. [1] among others.

An important component of this weak coupling methodology lies in the fact that in his procedure, Bielak et al. [1] do not make any hypothesis concerning the constitutive behavior of soil media. Consequently, the methodology can also be applied for nonlinear soil behavior as it was also demonstrated in the work of [4], [5], [17]. In a similar context as the one described through the DRM procedure, several authors have proposed structural zooms and sub-structuring methods in order to split the initial problem and study in a more detailed way a specific domain of interest [18]–[20].

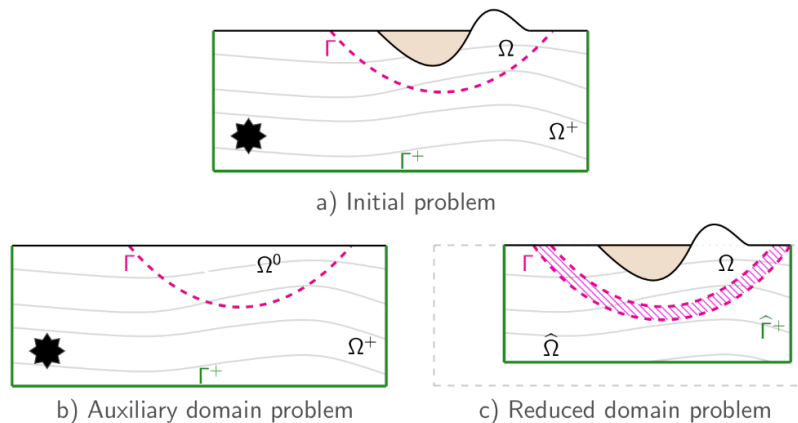


Fig. 1 - Schematic representation of the domain reduction method (adapted from [1]).

## 2.2 Implementation in code\_aster

In a finite element framework with code\_aster, the computation and application of the equivalent nodal forces is performed with the use of paraxial elements, which are located on the boundary of the reduced domain and facilitate the solution of the dynamic problem in the transient domain. Dynamic impedances are built locally in space and time on the boundary interface of the reduced domain using the zero-order paraxial approximation [13] and based on celerity values from the adjoining medium. The satisfaction of the paraxial approximation and the compatibility condition on the boundary is ensured by the continuity of the displacement  $\mathbf{u}_b$  and the stress vector  $\mathbf{t}_b$ , as it is demonstrated in [13], [21], [22]:



$$\begin{cases} \mathbf{u}_b + \mathbf{u}'_b = 0 \\ \mathbf{t}_b + \mathbf{t}'_b = 0 \end{cases} \quad (2)$$

The implemented version of paraxial elements in code\_aster is based in the methodology proposed by Modaressi [21] and Modaressi and Benzenati [23], where the elements are used in order to apply the dynamic excitation as well as to absorb the outgoing reflected waves on the boundary of the finite domain.

#### 4. Verification of implemented weak coupling

A numerical code using the spectral element method (SEM) is used in this section in order to study the wave propagation problem at a regional scale. SEM was initially introduced by Patera et al. [24] in order to study computational fluid dynamics problems, which is a modification of the finite element method by considering higher order polynomials as bases functions. The initial formulation of Patera et al. [24] adopts Chebyshev polynomials as bases functions, while in a further version Maday and Patera [25] proposed the use of Lagrange polynomials in conjunction with the Gauss-Lobatto-Legendre (GLL) quadrature, which leads to a diagonal mass matrix of the problem. The efficiency of the method for applications in seismology is presented in [26], [27], among others.

The weak coupling between a spectral element (SEM3D) and a finite element (code\_aster) is presented here without the presence of the structure. The verification of the methodology is initially provided for the simple canonical case of PRENOLIN [11], and then extended to the more complex case-study of CAN4 [12].

##### 4.1 Important hypothesis and coupling procedure

The implemented weak coupling between the SEM3D and code\_aster is presented here briefly. As showed before, it is based on the exchange of the displacement field  $\mathbf{u}_b$  and stress vector  $\mathbf{t}_b$  fields so as to assure the compatibility and continuity of the incident waves on the surface boundary of the reduced domain (see also Eq. (2)). Under this context, a surface boundary of a domain of interest is initially defined inside the SEM3D model (red line in SEM3D - Fig. 2). The necessary kinematic fields on a point of interest are exported for all the GLL points (blue points in Fig. 2) situated on this boundary. As a first approximation and due to the differences between the available traction vector of SEM and FEM, the kinematic fields are also exported on the neighboring nodes of a one element layer on the boundary of the reduced domain. These kinematic fields are then used in code\_aster in order to compute the stress vector at the interface (red line in code\_aster - Fig. 2). The aforementioned procedure is presented schematically in Fig. 2.

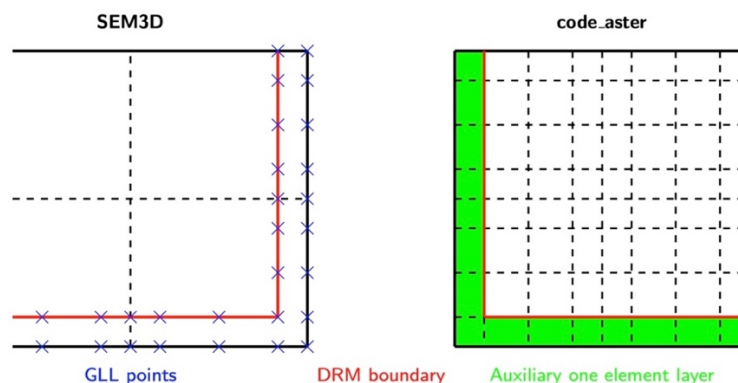


Fig. 2 - Schematic representation of the SEM/FEM weak coupling procedure.

For the studies presented in this work, the hypothesis of the conformity of the mesh between the two models is taken into consideration. Consequently, as depicted in Fig. 2, the mesh of the reduced domain in code\_aster is directly built from the GLL points where the fields are exported from SEM3D. Another important hypothesis is that the reduced domain is entirely included inside a homogeneous soil layer and thus no material



properties interpolation is necessary between the two numerical codes. Finally, in order to validate the weak coupling, the response of the reduced domain is going to be compared to the one obtained from a full SEM3D wave propagation analysis.

## 4.2 Canonical case-study: PRENOLIN

The canonical case-study inspired from the one of PRENOLIN benchmark [11] is examined at first. The dimensions of the soil domain are  $700 \times 700 \times 400 \text{ m}^3$  while the reduced domain, which is entirely included in the upper soil layer of the SEM3D model (red domain in Fig. 3) is a  $10 \times 10 \times 10 \text{ m}^3$  box. Dynamic excitation is applied in SEM3D as a plane wave in the x direction. Perfectly Matched Layers (PML) [28] are used as absorbing boundary conditions at SEM3D in order to avoid spurious reflections on the boundaries. Soil stratification and mechanical properties are presented in Fig. 3.

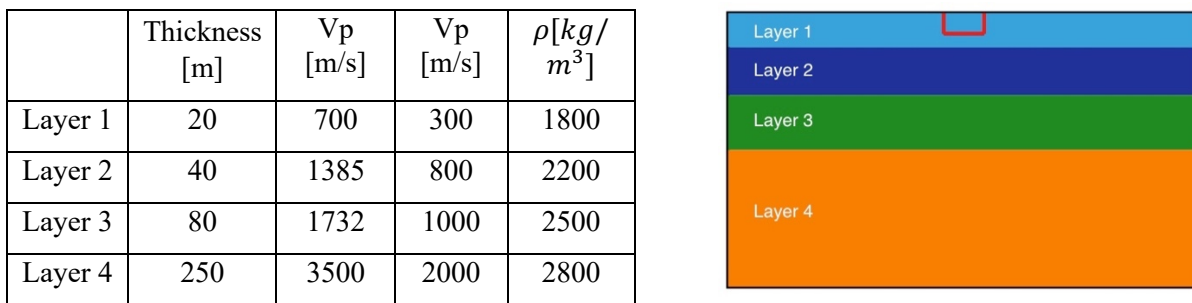


Fig. 3 - PRENOLIN: mechanical characteristics (left), geometry (right).

The comparison between the reference's response and the one obtained from the weak coupling is evaluated using Kristekova's criterion [29], [30]. This criterion compares the goodness-of-fit of the envelope between a signal of reference and a computed signal and provides a score in 0 to 10 scale. For a value equal to 10, a perfect correspondence is observed for the two signals. The mathematical expression of the criteria (Eq. (3)) is based on the energy distribution of a signal  $W$  in the time-frequency plane.

$$TFEM(t, f) = 10 \exp\left(-\frac{||W_i|| - ||W_{ri}||}{||W_{ri}||}\right) \quad (3)$$

where  $W_i, W_{ri}$ , are the energy distribution of the computed signal and the reference signal, respectively. The Kristekova's criterion is applied for accelerograms of several points in the surface of the reduced soil domain and the isosurface of the score is plotted in Fig. 4 (right). Perfect match is observed between the reference signal and the computed one. Equivalently, the comparison of the accelerogram for a point on the surface and at the center of the domain (Fig. 4(left)) shows as expected perfect correspondence between the two responses.

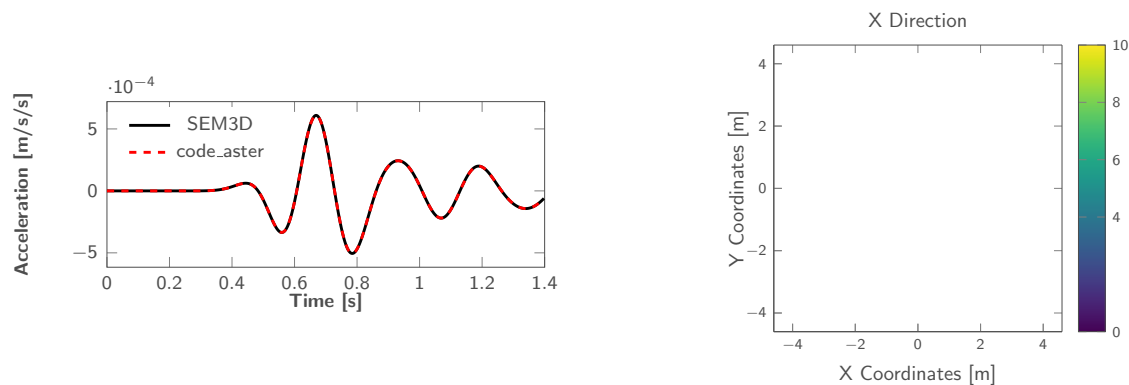


Fig. 4 - Weak coupling for the PRENOLIN case: accelerogram for a point at the center of the domain (left), isosurface of the Kristekova's criterion (right).



### 4.3 Canonical case-study: CAN4<sup>1</sup>

The second case to be examined is the canonical case-study of CAN4 [12]. It consists of a trapezoidal domain presented in Fig. 5(left), where the trapezoidal form of the basin aims to generate surface waves inside the soil domain. The dimensions of the model are  $22 \times 12 \times 6 \text{ km}^3$ , while the dimensions of the reduced domain are  $200 \times 200 \times 100 \text{ m}^3$ . Dynamic excitation is applied as a double-couple point source, which is situated at the center of the domain in an XY plane at  $3 \text{ km}$  depth. As in the previous case, perfectly matched layers are used on the boundaries of the SEM3D domain.

	Thickness [m]	Vp [m/s]	Vs [m/s]	$\rho$ [kg /m <sup>3</sup> ]
Soil	215	4500	650	2600
Rock	5785	4500	2600	2600

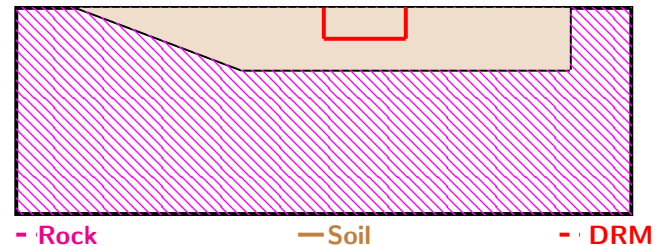


Fig. 5 - CAN4: mechanical properties (left) and geometry (right).

The isosurface of the Kristekova's criterion is plotted initially for all the points of the reduced domain's surface (Fig. 6). Differently from the previous case, we can now observe regions at the surface of the reduced domain where the reduced domain response is not the same as obtained from the auxiliary domain. Based on Fig. 6, these points are mainly situated in two symmetric regions with respect to the XZ axis while the worst value of the criterion is observed for a point on the middle of the domain.

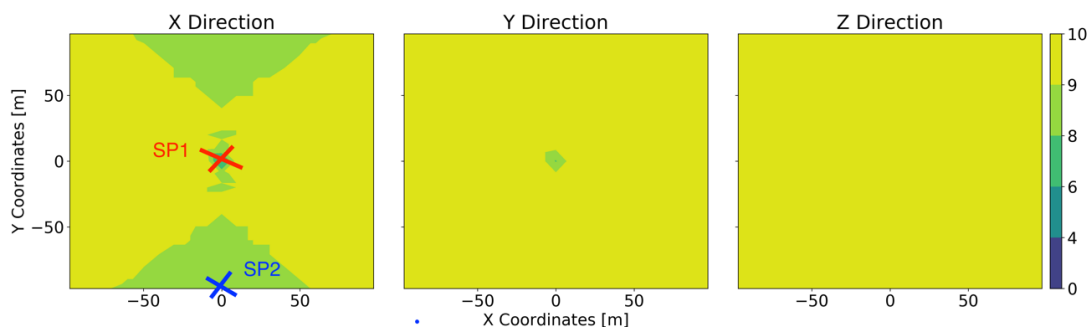


Fig. 6 - Isosurface of the Kristekova's criterion for the surface of the reduced domain.

In order to further examine the differences between the two responses, the accelerograms for points SP1, and SP2 (Fig. 6) are presented in Fig. 7. For the point SP1, which is located on the center of the domain (worst value of Kristekova's criterion) a difference is observed for the X and Y direction. However, absolute acceleration values at X and Y directions are 8 orders lower than Z direction, so the observed differences might be related to the numerical noise of the two different resolution methods and not of the coupling methodology.

<sup>1</sup> [http://www.sismowine.org/model/E2VP\\_Can4.pdf](http://www.sismowine.org/model/E2VP_Can4.pdf)

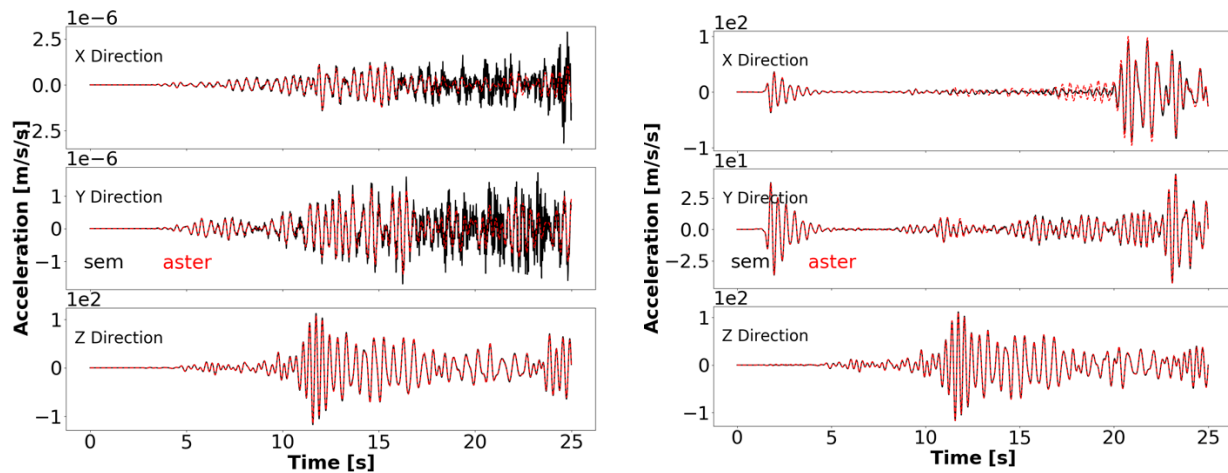


Fig. 7 - Accelerograms on soil surface: point SP1 (left), point SP2 (right).

A more significant difference is observed for the point SP2, which is situated on the boundary of the reduced domain (Fig. 6). The difference is localized after the first arrival of the seismic wave. A possible explanation of these discrepancies might be related to an inefficient absorption of outgoing surface waves via the paraxial elements in code\_aster.

The validation of a weak coupling between a spectral element and a finite element code was presented in this part. The coupling technique was tested for a linear elastic soil behavior and mesh conformity and the presented results allow us to validate the implemented procedure. Small differences were identified for the CAN4 case-study and a further investigation is necessary so as to pinpoint the source of the observed discrepancies. Different configurations of basin's geometry, as well as the variability of the source (position, magnitude, dimension) have to be taken into consideration so as to properly evaluate the DRM approach on the implemented coupling methodology. The question of material interpolation is also to be examined in future work.

### 3. Nonlinear DRM in code\_aster

The 3D seismic definition provided via the SEM/FEM weak coupling that was presented in the previous section can now be introduced as an input excitation of a finite-element numerical model for the study of nonlinear time-domain soil-structure interaction. However, in this work an evaluation of the DRM approach for the nonlinear soil behavior is only presented in a FEM/FEM weak coupling framework, where a simplified excitation of a plane wave is used to describe the “source” and the nonlinear case with a more complex 3D excitation is to be presented in a future work.

#### 3.1 Geometry and Mechanical characteristics

The case-study chosen for this analysis consist of a trapezoidal sedimentary basin enclosed in a rock domain. The geometry of the basin is the one of the Ohba valey proposed in [31] and presented in Fig. 8. The trapezoidal geometry of the basin is chosen so as to generate surface waves on the surface of the soil domain and thus to validate the efficiency of the DRM approach in the presence of such a type of waves. The dimensions of the soil domain are 400x400x92 m. The embedded structure that exists in the middle of the basin is the Unit 7 Reactor Building of the KARISMA benchmark [16]. Mechanical characteristics for the soil stratification as well as the structure are presented in Table 1.



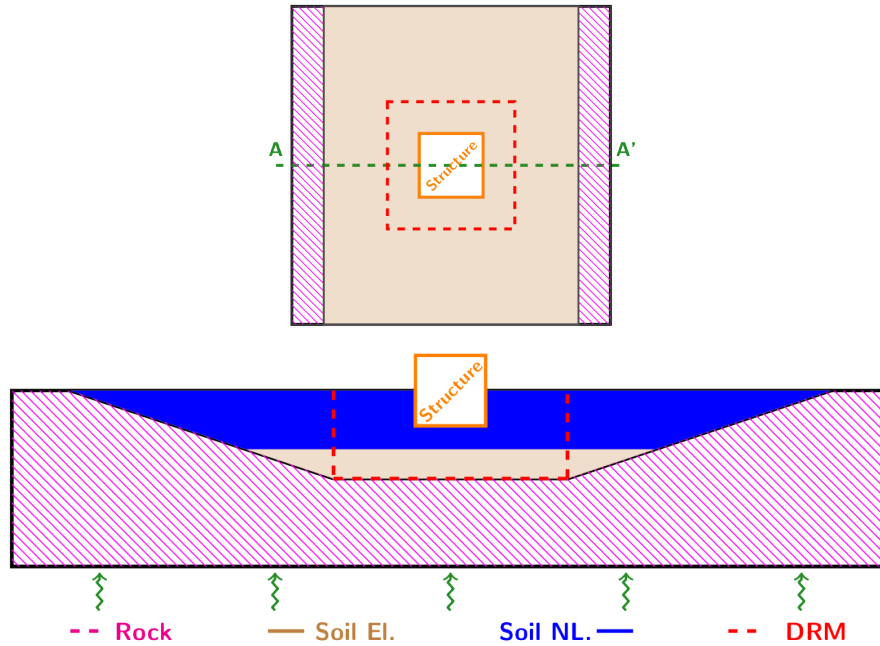


Fig. 8 - Geometry of the Ohba valley: XY view (top), XZ view (bottom).

Table 1 - Mechanical characteristics of the model.

	Thickness [m]	V <sub>s</sub> [m/s]	Poisson's Coefficient	ρ [kg/m <sup>3</sup> ]	Young's Modulus [GPa]	γ <sub>ref</sub>	n
<b>Soil</b>							
Layer 1	3.75	150	0.347	1710	$E = \frac{2 \times \rho \times V_s^2}{1 + \nu}$	$2.5 \times 10^{-4}$	0.7
Layer 2	3.75	200	0.308	1710		$2.5 \times 10^{-4}$	0.7
Layer 3	9.59	330	0.462	1730		$1. \times 10^{-3}$	1.0
Layer 4	29.96	490	0.451	1700			
Rock	45	530	0.446	1600			
<b>Structure</b>							
Concrete			0.2	2500	31.3		
Steel			0.3	7800	205		
Steel			0	0	192		

### 3.2 Numerical model, boundary conditions and loading

The numerical study presented in this paper supposes beams and shell finite elements for the modelling of structural elements and 3D volumetric elements for soil domain. Structure and soil are supposed to be elastic except from the upper layers of the basin (blue color in Fig. 8 – bottom) where Iwan's nonlinear constitutive law [15] is used in order to represent soil behavior. Iwan's law is an elasto-plastic multimechanism constitutive model for the description of deviatoric cyclic behavior of geomaterials, based on linear kinematic hardening. The volumetric part of deformations is supposed completely elastic and thus the yield surface is expressed in deviatoric stresses as:

$$f_n = q_n - Y_n \quad (4)$$



where  $Y_n$  is a constant providing the yielding limit for the  $n$  mechanism and  $q_n$  is the deviatoric stress associated with the same mechanism. Yielding limits  $Y_n$  and kinematic hardening parameters are computed through the degradation of the shear modulus  $G$  with the evolution of the shear deformation  $\gamma$ . This progressive degradation is obtained through the hyperbolic Eq. (5):

$$G = \frac{G_{max}}{\left(1 - \frac{\gamma}{\gamma_{ref}}\right)^n} \quad (5)$$

where  $G_{max}$  is the initial shear modulus,  $\gamma_{ref}$  is the shear deformation that generates  $G = G_{max}/2$  and  $n$  is the exponential of the hyperbolic law. The calibration of model parameters,  $\gamma_{ref}$  and  $n$ , is based on the the  $G - \gamma$  curves proposed by Seed and Idriss in 1971 [32] and the final values are presented in Table 1. A complete description of the model is presented in [15].

The dynamic loading for the initial problem is a vertical incident plane wave (SH, SV, P) applied at the base of the soil domain, where we apply all the three components of the acceleration simultaneously. The accelerograms that were used are the ones of the 2007 Niigata Chuetsu-Oki earthquake mainshock presented in [14]. Paraxial absorbing boundaries are used in the four lateral faces as well as the base of the model so as to avoid spurious reflections of the outgoing waves.

### 3.3 DRM procedure and numerical results

The DRM approach followed in this work is schematically presented in Fig. 9. The considered reference model is the auxiliary model used to compute the equivalent nodal forces on the boundary of the reduced domain. Therefore, the equivalent nodal forces  $\mathbf{F}_{eq}$  are the solution at the boundaries of the reduced domain and the soil and structure's response is expected to be the same on the reference and reduced domain.

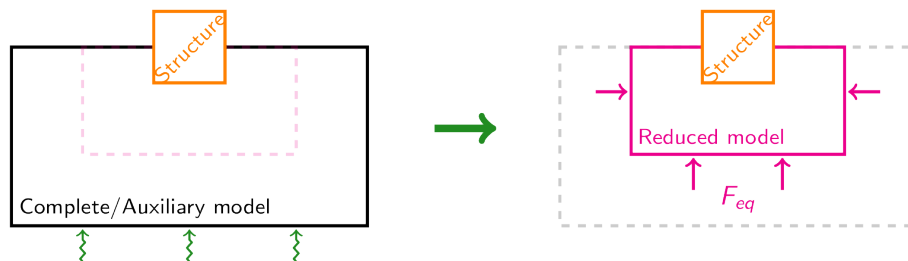


Fig. 9 - Schematic representation of the DRM approach.

Fig. 10 presents the comparison between the reference model and the reduced model for a point at the top of the structure. As expected, very good correspondence is observed between the two responses.

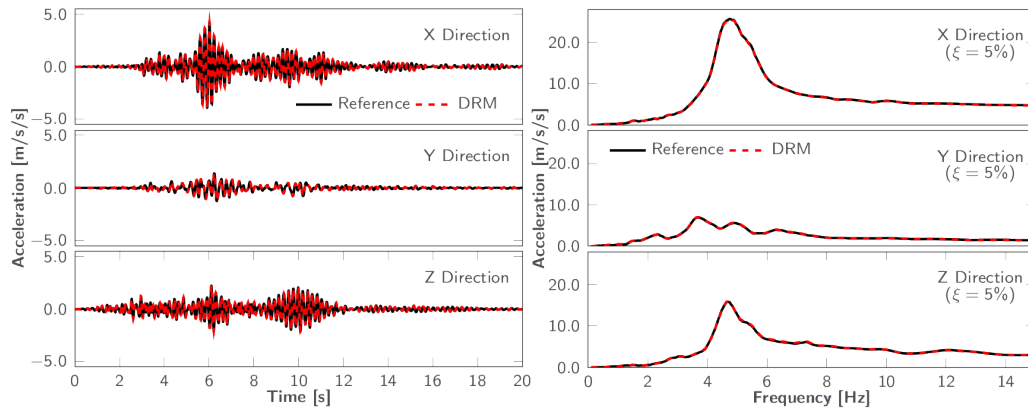


Fig. 10 - Comparison for the response of the structure (point at the top): accelerogram (left), response spectra (right)

In order to examine soil's response, the response spectra for different points at the surface of soil is presented in Fig. 11. The 3 points are taken at the soil surface and next to the structure on the Y axis (SP1), XY axis (SP2), and X axis (SP3). Again, good correspondence is observed between the reference solution and the reduced domain result.

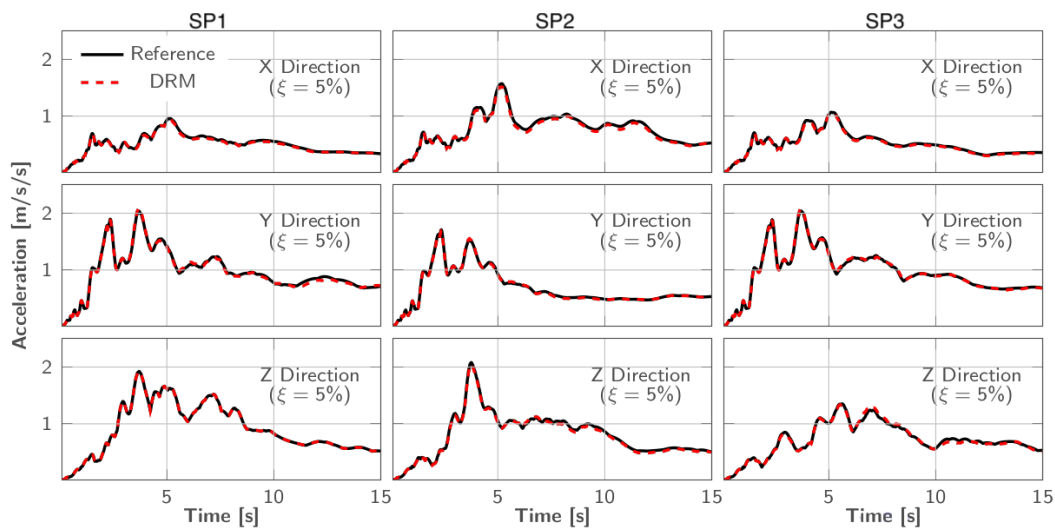


Fig. 11 - Response spectra for different points (next to the structure) at the surface of the soil.

## 5. Conclusions and Perspectives

The application of the domain reduction method (DRM) for a more accurate definition of the seismic input motion on soil-structure interaction studies is examined in this work. A SEM/FEM weak coupling between SEM3D and code\_aster is implemented in this work. The coupling was tested for a homogeneous reduced domain, boundary conform meshes and constant elastic properties at each soil layer. Two case studies with an increased complexity in terms of basin's geometry and seismic excitation are analyzed. For the given case-studies, the coupling procedure can be deemed successful. At a further step, the aspects of fields and material interpolation have to be examined in a high-performance computing framework, where the finite element model is going to be solved at a kilometric scale in order to also account for site effects.

For the second part of this work, the weak coupling in a finite-element framework is examined for the case study of the Karisma benchmark. The basin's form is modified so as to generate surface waves and



evaluate their impact in the efficiency of the method. The nonlinear Iwan's constitutive law is used to describe soil behavior. A good correspondence is observed between the reference domain and the reduced domain. However, the solution proposed in this work considers an auxiliary model that is same as the model of reference. An auxiliary model without the presence of the structure is going to be examined in future work in order to evaluate the efficiency of the DRM, on a SEM/FEM coupling framework.

## 6. Acknowledgements

The work presented in this paper was consists a part of the research activities supported by the SEISM Institut (<https://www.institut-seism.fr/>). The authors would also like to express their gratitude to the Association Nationale de la Recherche et de la Technologie (ANRT) for their financial support.

## 7. References

- [1] J. Bielak, C. Yoshimura, Y. Hisada, and A. Fernández, "Domain Reduction Method for Three-Dimensional Earthquake Modeling in Localized Regions, Part I: Theory," *Bull. Seismol. Soc. Am.*, vol. 93, no. 2, pp. 825–840, 2003, doi: 10.1785/0120010251.
- [2] B. Jeremić, G. Jie, M. Preisig, and N. Tafazzoli, "Time domain simulation of soil-foundation-structure interaction in non-uniform soils," *Earthq. Eng. Struct. Dyn.*, vol. 38, no. 5, pp. 699–718, Apr. 2009, doi: 10.1002/eqe.896.
- [3] E. Sáez, F. Lopez-Caballero, and A. Modaressi-Farahmand-Razavi, "Effect of the inelastic dynamic soil-structure interaction on the seismic vulnerability assessment," *Struct. Saf.*, vol. 33, no. 1, pp. 51–63, 2011, doi: 10.1016/j.strusafe.2010.05.004.
- [4] J. M. Solberg, Q. Hossain, and G. Mseis, "Nonlinear time-domain soil–structure interaction analysis of embedded reactor structures subjected to earthquake loads," *Nucl. Eng. Des.*, vol. 304, pp. 100–124, Aug. 2016, doi: 10.1016/j.nucengdes.2016.04.026.
- [5] H. Wang, H. Yang, S. K. Sinha, and C. Luo, "3-D Non-Linear Earthquake Soil-Structure Interaction Modeling of Embedded Small Modular Reactor (SMR) Different Sources of Energy Dissipation in Soil Structure Interaction System View project Multi-scale study on the deformation and failure mechanism of granular materials View project."
- [6] V. A. Fernandes *et al.*, "Dynamic soil-structure interaction modeling strategies applied to Kashiwazaki-Kariwa nuclear power plant case-study," *COMPADYN 2017 - Proc. 6th Int. Conf. Comput. Methods Struct. Dyn. Earthq. Eng.*, vol. 1, no. June, pp. 2330–2342, 2017, doi: 10.7712/120117.5571.17197.
- [7] I. Zentner and G. Devésá, "A methodology for soil-structure interaction analysis accounting for spatially incoherent seismic free field motion," *Proc. 8th Int. Conf. Struct. Dyn. EUROSDYN 2011*, no. February 2015, pp. 589–594, 2011.
- [8] R. Cottreau, D. Clouteau, and C. Soize, "Probabilistic impedance of foundation: Impact of the seismic design on uncertain soils," *Earthq. Eng. Struct. Dyn.*, vol. 37, no. 6, pp. 899–918, May 2008, doi: 10.1002/eqe.794.
- [9] "SEM3D Registered at French Agency for Protection of Programs (Dépôt APP)." CEA, CentraleSupélec, IPGP & CNRS.
- [10] "Code\_Aster General public licensed structural mechanics finite element software, included in the Salomé-Méca simulation platform."
- [11] J. Régnier *et al.*, "Prenolin: International benchmark on 1D nonlinear: Site-response analysis—validation phase exercise," *Bull. Seismol. Soc. Am.*, vol. 108, no. 2, 2018, doi: 10.1785/0120170210.
- [12] "E2VP-2 - EuroSeistest Verification and Validation Project - CAN4 : simplified model of the Mygdonian basin, homogeneous layers inside the basin," 2011.
- [13] Code\_Aster, "General public licensed structural mechanics finite element software, included in the Salomé-Méca simulation platform. Website <http://www.code-aster.org>. En particulier : [R4.02.05] Éléments de frontière absorbante," 2017.



- [14] M. Korres, F. Gatti, V. Alves Fernandes, F. Lopez-Caballero, I. Zentner, and F. Voldoire, “Impact de la définition du mouvement sismique 3D à l’aide d’un modèle physique sur les études d’interaction sol- structure,” in *10ème Colloque National AFPS2019*, 2019.
- [15] Code\_Aster, “General public licensed structural mechanics finite element software, included in the Salomé-Méca simulation platform. Website <http://www.code-aster.org>. En particulier: [R7.01.38] Loi d’Iwan pour le comportement cyclique de matériaux granulaires,” 2017.
- [16] IAEA/TECDOC-1722, “Review of Seismic Evaluation Methodologies for Nuclear Power Plants Based on a Benchmark Exercise,” no. November 2013, 2013.
- [17] J. Bielak and P. Christiano, “On the effective seismic input for non-linear soil-structure interaction systems,” *Earthq. Eng. Struct. Dyn.*, vol. 12, no. 3, pp. 107–119, 1984, doi: 10.1002/eqe.4290120108.
- [18] R. W. Clough and E. L. Wilson, “Dynamic analysis of large structural systems with local nonlinearities,” *Comput. Methods Appl. Mech. Eng.*, vol. 17–18, pp. 107–129, Jan. 1979, doi: 10.1016/0045-7825(79)90084-7.
- [19] I. Hirai, Y. Uchiyama, Y. Mizuta, and W. D. Pilkey, “An exact zooming method,” *Finite Elem. Anal. Des.*, vol. 1, no. 1, pp. 61–69, 1985, doi: 10.1016/0168-874X(85)90008-3.
- [20] J. De Mersseman, “APPLICATION DE LA MÉTHODE DE SOUS-STRUCTURATION GRAVOUIL-COMBESURE DANS LE CADRE DE L’ISS,” 2017.
- [21] H. Modaressi, “Modélisation numérique de la propagation des ondes dans les milieux poreux anelastiques,” Ecole centrale de Paris, 1987.
- [22] F. De Martin, H. Modaressi, and H. Aochi, “Coupling of FDM and FEM in seismic wave propagation,” in *4th International Conference on Earthquake Geotechnical Engineering*, 2007.
- [23] H. Modaressi and I. Benzenati, “An absorbing boundary element for dynamic analysis of two-phase media,” in *10th World Conf. on Earthquake Engineering*, 1992, pp. 1157–1163.
- [24] A. T. Patera, “A spectral element method for fluid dynamics: Laminar flow in a channel expansion,” *J. Comput. Phys.*, vol. 54, no. 3, pp. 468–488, 1984, doi: 10.1016/0021-9991(84)90128-1.
- [25] A. T. Maday, Yvon and Patera, “Spectral element methods for the incompressible Navier-Stokes equations,” in *State-of-the-art surveys on computational mechanics (A90-47176 21-64)*. New York, American Society of Mechanical Engineers, 1989, pp. 71–143.
- [26] D. Komatitsch, “Méthodes spectrales et éléments spectraux pour l’équation de l’élastodynamique 2D et 3D en milieu hétérogène,” pp. 1–188, 1997.
- [27] D. Komatitsch and J.-P. Vilotte, “The Spectral Element Method: An Efficient Tool to Simulate the Seismic Response of 2D and 3D Geological Structures.”
- [28] J.-P. Berenger, “A perfectly matched layer for the absorption of electromagnetic waves,” *J. Comput. Phys.*, vol. 114, no. 2, pp. 185–200, Oct. 1994, doi: 10.1006/jcph.1994.1159.
- [29] M. Kristeková, J. Kristek, P. Moczo, and S. M. Day, “Misfit criteria for quantitative comparison of seismograms,” *Bull. Seismol. Soc. Am.*, 2006, doi: 10.1785/0120060012.
- [30] M. Kristeková, J. Kristek, and P. Moczo, “Time-frequency misfit and goodness-of-fit criteria for quantitative comparison of time signals,” *Geophys. J. Int.*, 2009, doi: 10.1111/j.1365-246X.2009.04177.x.
- [31] F. Gelagoti, R. Kourkoulis, I. Anastasopoulos, T. Tazoh, and G. Gazetas, “Seismic wave propagation in a very soft alluvial valley: Sensitivity to ground-motion details and soil nonlinearity, and generation of a parasitic vertical component,” *Bull. Seismol. Soc. Am.*, vol. 100, no. 6, pp. 3035–3054, Dec. 2010, doi: 10.1785/0120100002.
- [32] I. M. Seed, Harry Bolton and Idriss, “Simplified procedure for evaluating soil liquefaction potential,” *J. Soil Mech. & Found. Div.*, 1971.